

Summer Vacation 2003 – ASF Spatial Mapping in CO, AR, FL, and CA

Gregory Johnson, Ruslan Shalaev, *John J. McMullen Associates*
Richard Hartnett, *United States Coast Guard Academy*
Peter F. Swaszek, Todd Moyer, *University of Rhode Island*

Biographies

Gregory W. Johnson is a Program Manager for John J. McMullen Associates, responsible for contracts for the Coast Guard R&D Center in Groton, CT. One of the principal projects he is currently working on is providing research assistance to the Coast Guard Academy. Mr. Johnson holds a BSEE from the Coast Guard Academy (1987), a MSEE from Northeastern University (1993), and is currently working toward a Ph.D. at the University of Rhode Island.

Richard J. Hartnett received the BSEE. degree from the U. S. Coast Guard Academy (USCGA) in 1977, the MSEE degree from Purdue in 1980, and the Ph.D. EE from the University of Rhode Island in 1992. He holds the grade of Captain in the U. S. Coast Guard, and is Head of Electrical and Computer Engineering at the USCG Academy. CAPT Hartnett has been a faculty member at USCGA since 1985, and is serving as National Marine Representative, Institute of Navigation (ION) Council.

Peter F. Swaszek is a Professor of Electrical and Computer Engineering at the University of Rhode Island. He received his Ph.D. in Electrical Engineering from Princeton University. His research interests are in digital signal processing with a focus on digital communications systems.

Abstract

The Federal Aviation Administration (FAA) observed in its recently completed Navigation Transition Study that Loran-C, as an independent radionavigation (RNAV) system, is theoretically the best backup for the Global Positioning System (GPS). However, the FAA also observed that Loran-C's potential benefits to aviation hinges upon its ability to support non-precision approaches (NPA's), which mandates a Required Navigation Performance (RNP) of 0.3. Through FAA sponsoring, the U.S. Coast Guard Academy (USCGA) is responsible for conducting some of the tests and evaluations to help determine whether Loran can provide the accuracy, availability, integrity, and continuity to support NPA's in the National Air Space (NAS). A major part of assessing the suitability of Loran is in understanding the nature of Loran ground wave propagation over paths of varying conductivities and terrain. Propagation time adjustments, called "additional secondary factors (ASFs)," are used to adjust receiver times of arrival (TOAs) to account for propagation over non-seawater path(s). These ASFs vary both spatially and temporally, and unless understood and/or modeled, we lose accuracy and may not be able to guarantee a hazardously misleading information (HMI) probability of less than 1×10^{-7} . The Coast Guard Academy, with flight support from the FAA Technical Center, has been conducting a series of tests to measure ASF variations in the vicinity of several selected airfields in Colorado, Arkansas, Florida, and California. During these tests we measured ASFs during flights in the vicinity of selected airfields and we measured ASFs on the ground employing

mobile units at varying distances from the airfield. To factor out temporal variations in ASFs, we took measurements from a static monitor installed at each airfield, thereby allowing us to measure spatial variations in ASF relative to that monitor site. In another FAA sponsored effort, the University of Wales at Bangor has developed an ASF modeling program (BALOR). Predicted ASFs for these airfields were generated using BALOR and compared to the measured values.

Introduction

The Federal Aviation Administration (FAA) observed in its recently completed Navigation and Landing Transition Study [1] that Loran-C, as an independent radio navigation (RNAV) system, is theoretically the best backup for the Global Positioning System (GPS). However, this study also observed that Loran-C's potential benefits hinge upon the level of position accuracy actually realized (as measured by the 2 drms error radius):

- for aviation applications this is the ability to support non-precision approach (NPA) at a Required Navigation Performance (RNP) of 0.3 which equates to a 2 drms error of 309 meters
- for maritime applications this is the ability to support harbor entrance and approach (HEA) requirements which equates to a 2 drms error of 8-20 meters.

A significant factor in the accuracy of a Loran system is the spatial and temporal variation in the times of arrival (TOAs) observed by the receiver and presented to the position solution algorithm (so called ASFs, additional secondary factors) [2]. Hence, a key component in evaluating the utility of Loran as a GPS backup is a better understanding of ASFs and a key goal is deciding how to mitigate the effects of ASFs to achieve more accurate Loran-C positions while ensuring that the possibility of providing hazardous and misleading information (HMI) will be no greater than 1×10^{-7} . The U.S. Coast Guard Academy, as a part of the FAA's government, industry, and academia team, is striving to improve the understanding of the temporal, spatial, and directional variations in time of arrival (TOA) that could be mitigated. The intent is to develop a "differential" or enhanced Loran system that estimates and removes these ASFs to allow for higher precision position solutions.

Our Loran system for 2003 and beyond is based on a multi-station, multi-chain, all-in-view, DSP-based receiver observing TOA measurements with an H-field antenna. To improve performance, this new system separates the "ASF errors" (where this "ASF error" includes all TOA errors) into spatial, temporal, and directional components and uses a grid approach rather than waypoints. Specifically, as described in [3], our approach is to model each of the three components of the ASF errors, estimate parameter values for the models, and then "correct" the TOA observations using the models before applying the position solution algorithm.

For an aviation receiver the approach is to use a single set of ASF values (one for each Loran tower) for a given airport. This value may have seasonal adjustments applied to it. The Loran receiver will use this set of static ASF values to improve position accuracy when conducting a non-precision approach (NPA). The issue to be resolved is whether the ASF gradients are sufficiently small in the location of a given airport that use of a single static value will meet RNP 0.3 requirements. However, measuring gradients at every airport would be very time-consuming.

Under a separate research effort an ASF modeling tool has been developed by the University of Bangor which will hopefully allow ASF gradients to be predicted with sufficient accuracy. This paper addresses a series of tests conducted during the summer of 2003 to assess ASF gradients near selected airports and to compare measured ASF gradients to those predicted using the model in order to determine the feasibility of using the model instead of measurements. Subsequent sections further describe our ASF measurements and comparisons to the model.

Experiment Description

A number of areas were selected by the Loran Integrity and Performance Panel (LORIPP) to cover a representative sample of different topographies. Of these eight areas only four were used for the testing as there was insufficient time to make measurements at all. At each area, several airports in the vicinity were selected for the flight trials. The areas and airports for each area are listed in Table 1 along with the airport code (three-letter designator), a total of ten airports in four States. Figure 1 shows an overview of the flight tracks to each area and the flights at each area. The four areas are highlighted. The photos in Figures 2-5 give an idea of the terrain in each area; very mountainous in Grand Junction (figure 2), flat in Little Rock (Figure 3), flat and coastal in Pensacola (Figure 4), and flat coastal with nearby mountains inland in Monterey (Figure 5).

Table 1 – Areas and airports used for flight testing

| Colorado | Airport Code |
|----------------------------------|---------------------|
| Grand Junction – Walker Field | GJT |
| Montrose Regional | MTJ |
| Rifle – Garfield County Regional | RIL |
| Arkansas | |
| Little Rock – Adams Field | LIT |
| Hot Springs Memorial | HOT |
| Florida | |
| Pensacola Regional | PNS |
| Panama City | PFN |
| California | |
| Monterey Peninsula | MRY |
| Salinas Municipal | SNS |
| Watsonville Municipal | WVI |

In order to assess the ASF gradients, three types of data were collected; flight testing, ground mobile data, and ground static data. Each of these is described in the following sections.

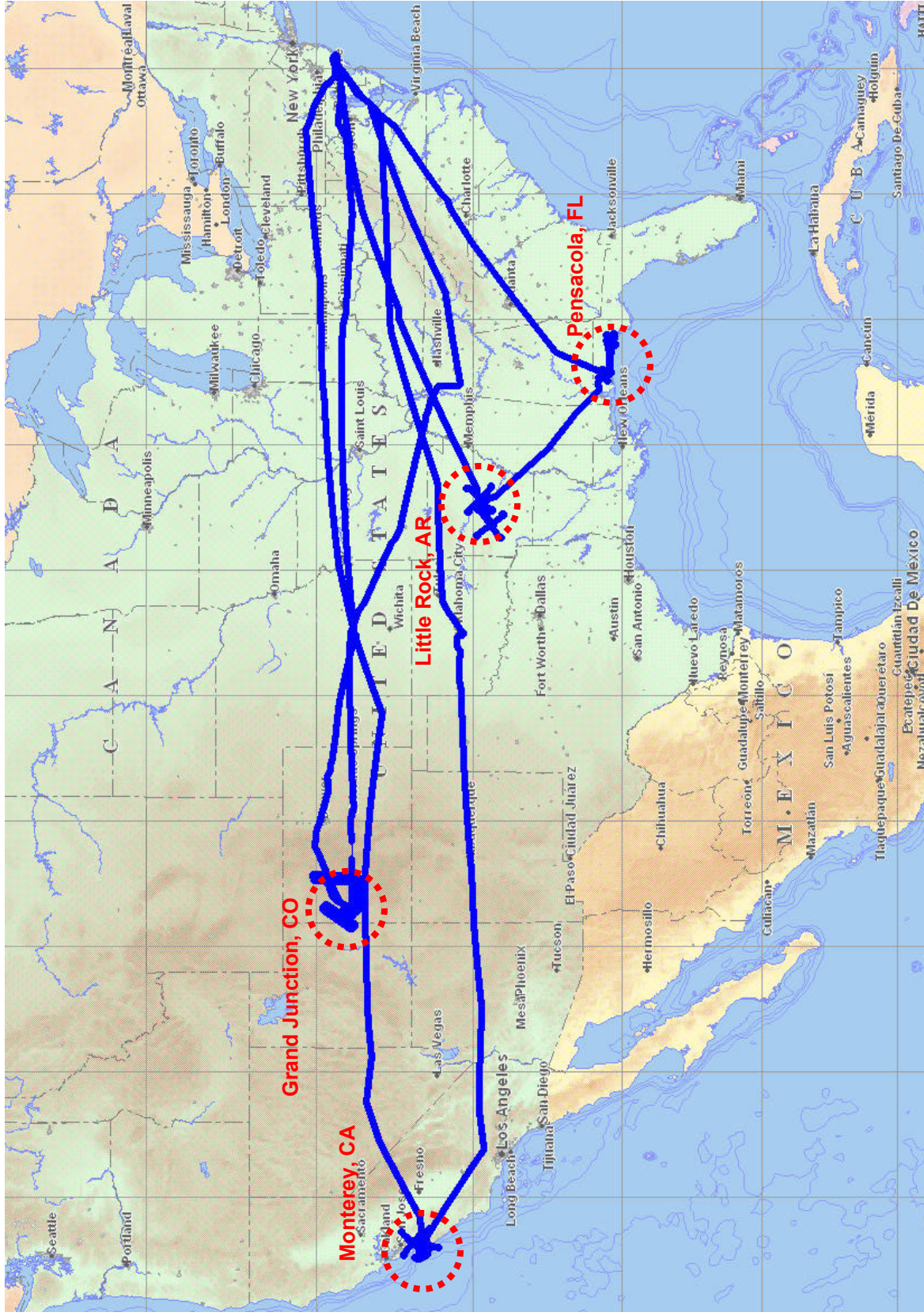


Figure 1 – Flight tracks for summer 2003 ASF mapping; the 4 test areas are circled and labeled in red



Figure 2 – Grand Junction, CO



Figure 4 – Pensacola, FL



Figure 3 – Little Rock, AR



Figure 5 – Monterey, CA



Figure 6 – FAA Convair 580

Flight Data

The first goal of the in-flight data was to measure ASF variations in the vicinity of the airports. The aircraft could cover more territory much more quickly than making measurements on the ground, but at less accuracy due to the flight speed and the increased noise on the aircraft. The original pattern used for this was a large oval (race track). This was done to keep the flights on only two pairs of reciprocal headings in order to reduce the influence of the directional variation problem with the H-field antenna (see our companion paper presented at the same conference for a discussion of this problem) [4]. In later flights the oval pattern was collapsed down to a cross pattern.

The second goal was to fly approaches for later post-processing of the TOA data with the static ASFs added. At each airport four approaches were flown.

The aircraft equipment consisted of two systems: a Locus SatMate 1020 receiver and a US Coast Guard Academy DDC-based ASF collection system. Both systems ran off of H-field aviation antennas. The Locus SatMate 1020 receiver was controlled by a USCGA/JJMA program that simultaneously captures the TOA information from the SatMate and GPS information from a NovAtel WAAS GPS receiver. This gives the GPS position for each Loran position, to the nearest 0.1 second. A diagram of the DDC-based ASF collection system is shown in Figure 7 and a photo of both systems installed on the Convair 580 is shown in Figure 8. This system is mostly the same as the mobile system described in our previous work [5]. The only difference is the replacement of the CGA developed EISA-board RF front end with a commercial amplifier/filter bank; the Frequency Devices 90IP. The operation, and calculation of ASFs is as previously described in [3, 5].

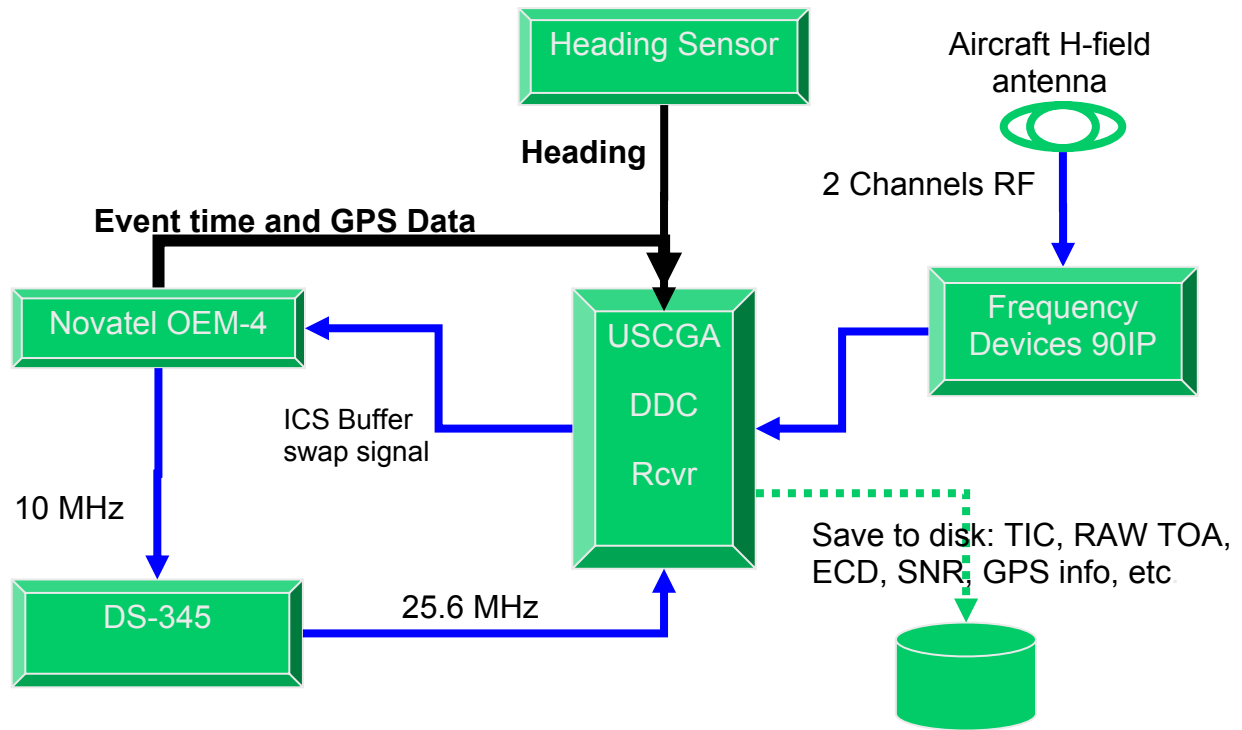


Figure 7 – Airborne ASF mapping system



Figure 8 – Photo of airborne ASF mapping system onboard Convair 580

Ground Mobile Data

Since it was not clear how accurate the airborne data would be, ASF data was also collected on the ground. The goal was to collect ASF data at static locations around each airport out to 25 NM. The ASF collection system was mounted in a car and moved from location to location. At each location, data was collected while stationary for about 15 minutes thus allowing for averaging to improve measurement accuracy. This data could then be used to assess ASF gradients and also used as a reference to assess the accuracy of the flight measurement data.

A diagram of the ground mobile equipment is shown in Figure 9, and a photo of the equipment mounted in a van is in Figure 10. The system operates in the same manner as the airborne system; however the form-factor is a little different. In order to reduce size and power demands, a single-box DC-powered system was developed. A custom Brandywine Synchclock32 PCI board with an Ashtech DG16 GPS receiver daughtercard was used to provide the time-tagging of the buffer swap signal and the GPS position and time. A new RF front end was developed on a PCI-board using Frequency Devices D83S programmable gain modules and filters. This was integrated with a digital I/O board to allow software control of the gain setting. The whole system was built in a DC-powered computer to allow for operation in a vehicle without an inverter.

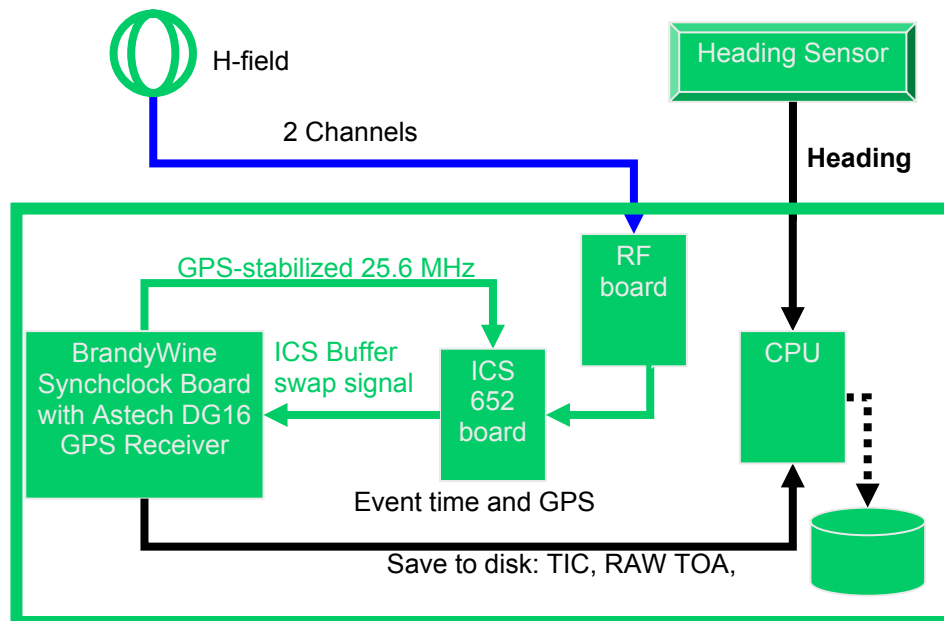


Figure 9 – Mobile (ground) ASF mapping system



Figure 10 – Photo of mobile ASF mapping system (circled in yellow) mounted in a van

Ground Reference Station

In order to factor out the temporal variations in the ASFs a ground reference station was used. This system was installed at the base airport in each area and operated continuously while collecting airborne and ground-mobile data. This concept has been described before in [5].

The equipment used for this reference station consisted of two independent systems, a USCGA DDC-based ASF measurement system and a Locus LRSIIID-based system. The DDC-based system is exactly the same as used in the aircraft (described above). A diagram of the LRSIIID-based system is shown in Figure 11. This is the same system as previously described in [5] though a number of improvements and refinements have been made to the USCGA/JJMA developed Locus-NovAtel integration software. Both of these systems were mounted in a rack in a waterproof box so that the system could be deployed into the field more easily; see Figure 12 for a photo of the box.

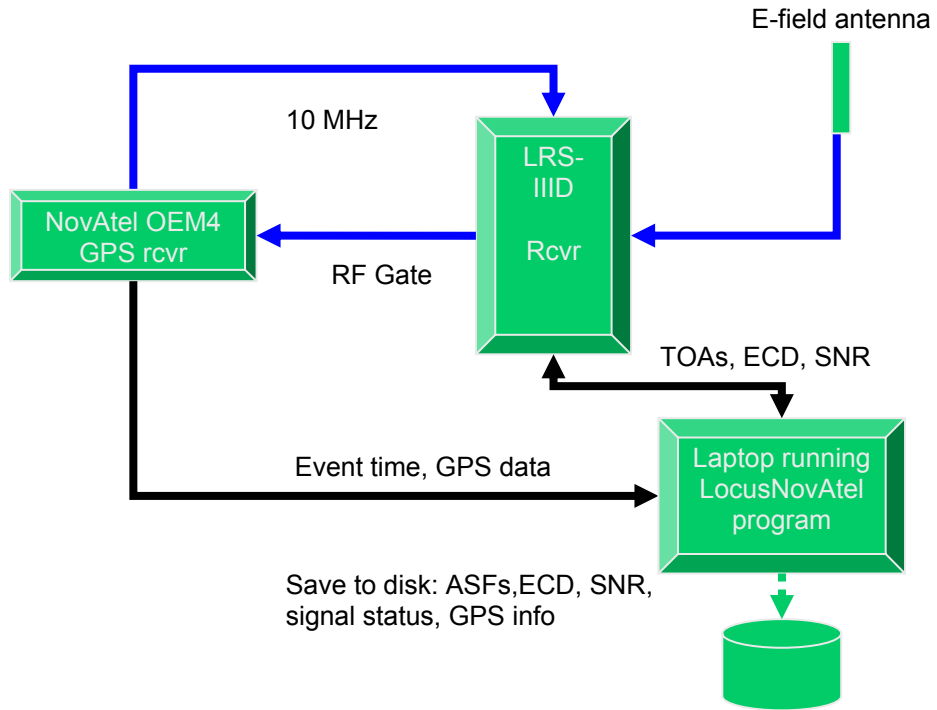


Figure 11—Ground reference station – Locus-NovAtel system



Figure 12 – Photo of ground reference station

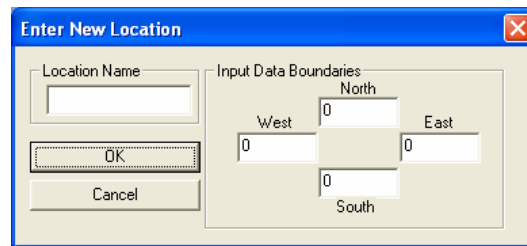
ASF gradients near airports/locales

BALOR Model

The University of Wales at Bangor has developed ASF prediction software called BALOR. This software was modified under an FAA-funded contract and delivered to the Loran Evaluation team. This software is designed for calculating predicted Additional Secondary Factors (ASFs) using the Monteath method [6, 7]. It uses a terrain elevation database (DTED Level 1 format), a ground conductivity database (from the FCC), and a coastline database (World Vector Shorelines) for the ASF computations.

BALOR Operation

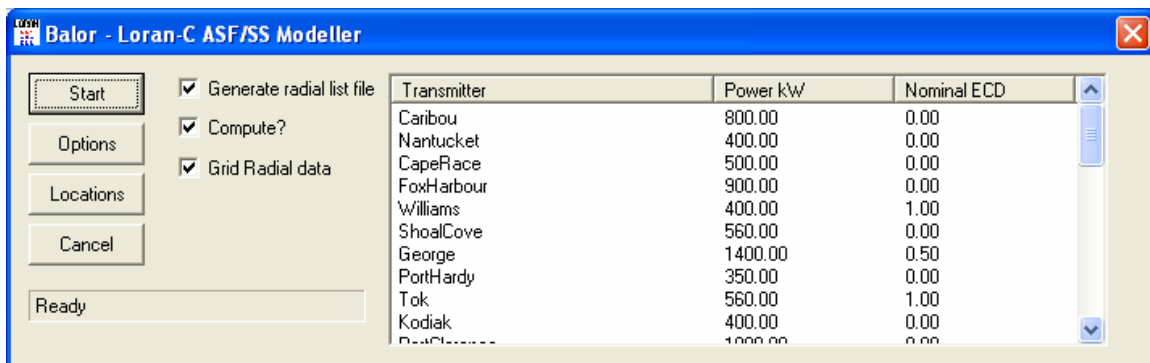
To compute a grid of ASF values the user specifies a rectangular area by inputting north, south, east and west boundaries:



The user also sets the height of the receiver off the ground and latitude/longitude resolution (grid points spacing) of the output ASF grid. It was observed that at resolution set below 0.001 degree, BALOR in some instances produced erroneous predicted ASF values - 0, 999 and -999:



After setting options the user selects the transmitting station and runs the predicted ASF calculations:



The resulting predicted ASF grid is written into a 3 column tab-delimited text spreadsheet with latitude/longitude in the first two columns and the ASF values in the third column:

```
34.688 34.689 -92.304 -92.303 0.001 0.001
34.6880 -92.3040 -6.0713
34.6880 -92.3030 -6.0670
34.6890 -92.3040 -6.0671
34.6890 -92.3030 -6.0712
```

BALOR Usage

For modeling airborne predicted ASF data, calculations were run for a grid covering the area where flight patterns were flown. One difficulty leading to possible inaccuracy in the results is that actual flight patterns were flown at a fixed altitude (relative to sea level), but in BALOR, it is only possible to specify the receiver height relative to the ground. In some areas, such as Grand Junction, the aircraft height above ground varied considerably due to the terrain. To account for that limitation, calculations were performed twice for each area– at the ground level and at an average flying height relative to the ground. Patterns were computed with longitude and latitude resolutions set to 0.01 degree.

For modeling fixed locations, custom software was written to extract lists of locations from spreadsheets generated during the Matlab analysis of the measured data and write them into BALOR “.loc” receiver location files. BALOR allows for a maximum resolution of 0.001 degree and does not allow calculating predicted ASF values for a single location, only for grids. To work around this limitation, actual receiver locations were rounded up and rounded down to a thousandth of a degree to produce a bounded 4-point-grid for each actual location. After running predicted ASF calculations on those grids, custom BALOR data-processing software was used to combine BALOR output data files (separate directory/files for each station/location pair) into a single text file and to match locations/predicted ASFs/Stations from that file with locations in the original spreadsheets and insert predicted ASF values into appropriate columns.

BALOR Plots

Some typical BALOR output grids are show in Figures 14 thru 17. These are predicted ASF grids for the area near the Montrose airport in Colorado and cover the area of the oval racetrack flight pattern. There are two grids, one calculated with the receiver height set at ground level (Figures 14 and 15) and one with the receiver height set at 9700 ft (Figures 16 and 17) as that is the height of the aircraft above ground at Montrose airport. For each grid there are two representations of the same data; a 3D mesh plot (Figures 14 and 16) and a colored contour plot (Figures 15 and 17). Comparing Figures 15 and 17 you can see slight differences in the calculations for ground level vs. at 9700 ft.

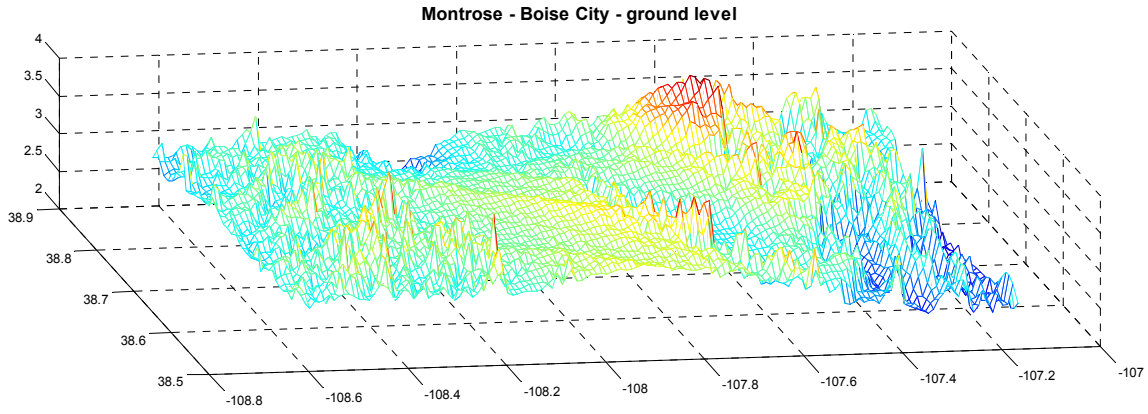


Figure 14 – BALOR grid for area near Montrose airport at ground level, 3D mesh plot

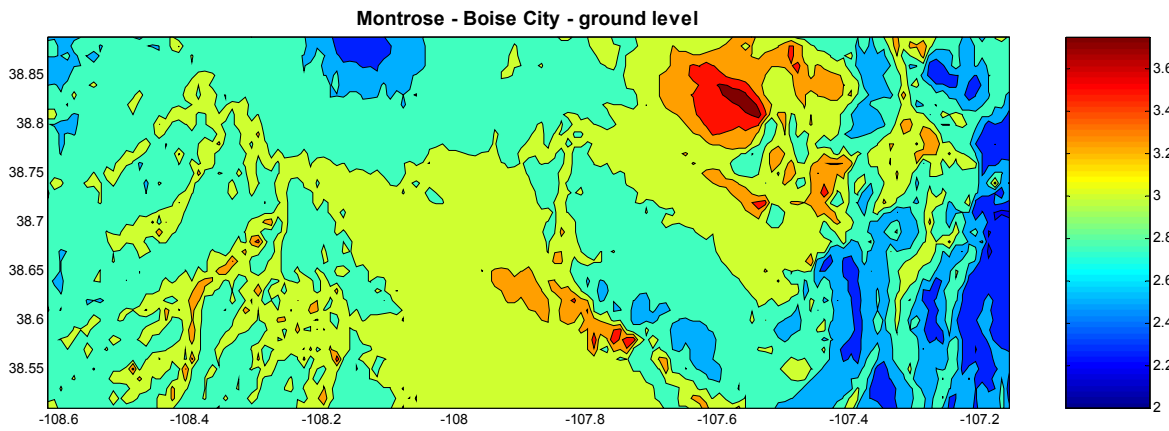


Figure 15 -- BALOR grid for area near Montrose airport at ground level, contour plot

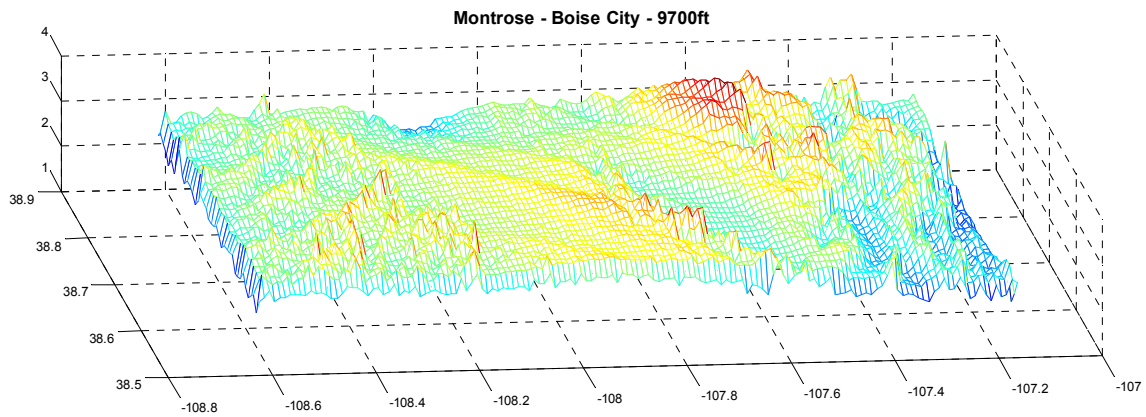


Figure 16 -- BALOR grid for area near Montrose airport, 9700ft above ground, 3D mesh plot

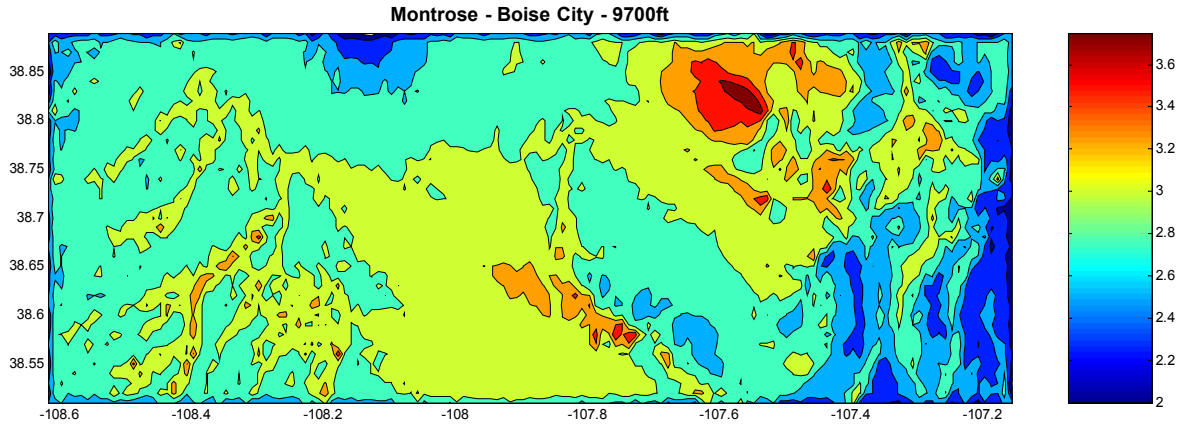


Figure 17 -- BALOR grid for area near Montrose airport, 9700ft above ground, contour plot

The map in Figure 18 shows a view of the Colorado test area. The flights near Grand Junction, Montrose, and Rifle are plotted in yellow, red, and green respectively. The blue flags indicate the locations that ground data was collected at. The BALOR grids above cover the area of the red oval (flight near Montrose). Figure 19 is a close-up on just this area and also shows the mountainous terrain.

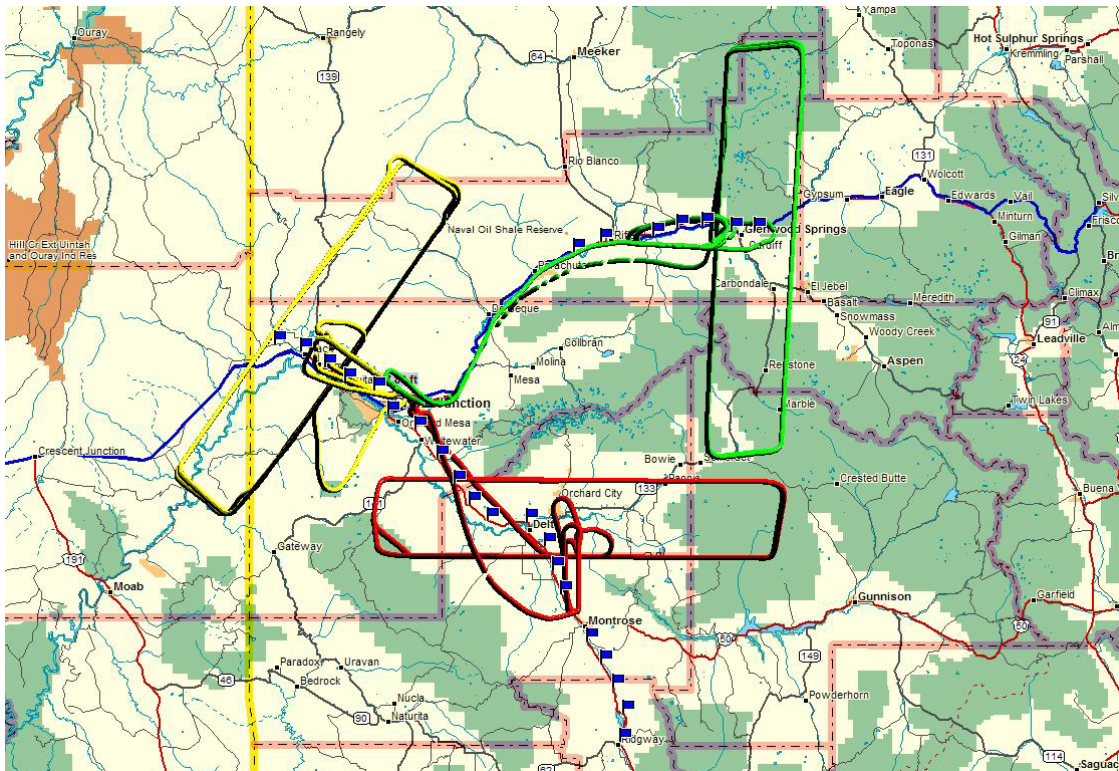


Figure 18 – ASF measurements in Colorado. Red, yellow, and green are the 3 flights; blue flags are the ground measurement locations

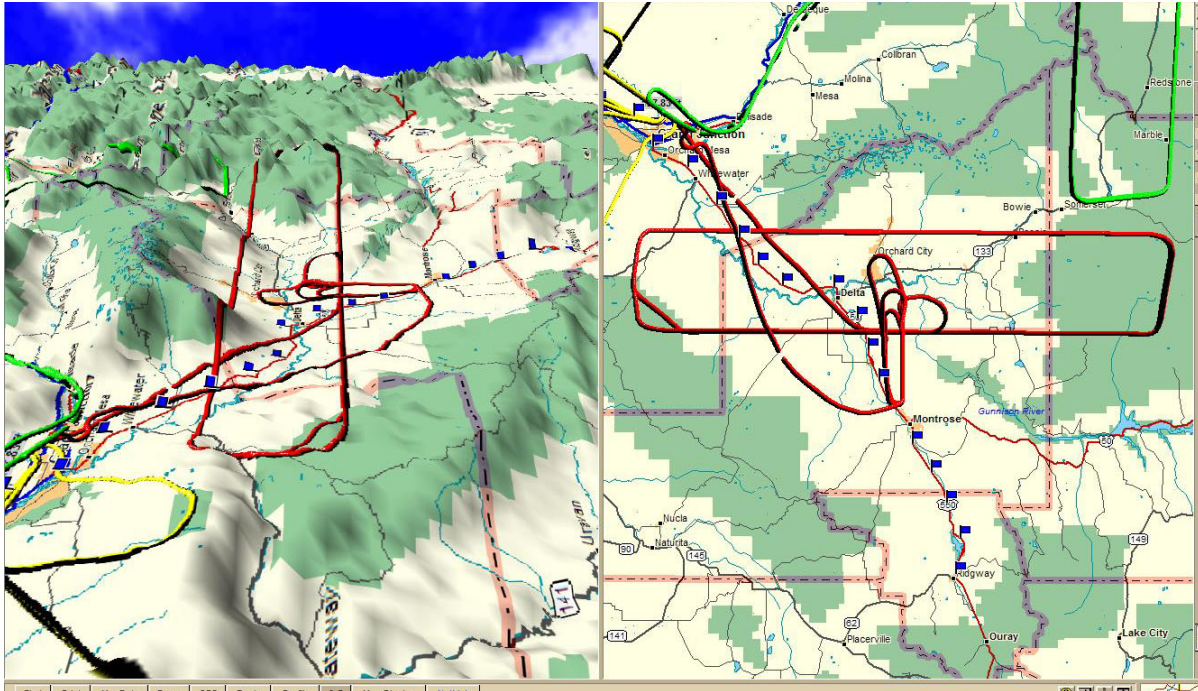


Figure 19 – Close-up of Montrose area flight track, left-hand view shows the topography (looking from the East to the West)

Results

Relative TOA Definition

In the typical definition, TOA ASFs are the additional propagation delay due to a non-seawater path. This additional time delay is a function of the terrain and conductivity along the path the signal takes between the Loran tower and the receiver. This value is very difficult to measure directly. When the receiver makes a precise TOA measurement relative to UTC at a known location, the predicted (all-seawater path) TOA can be subtracted off leaving the ASF. However, this difference is corrupted by system timing errors which mask the true ASF value; let's call this corrupted ASF, ASF^*

Our approach to resolving this has been to calculate relative ASFs. At each location where we made TOA/ASF measurements, we also collected ASF measurements at a fixed reference location. These values are also corrupted by system timing errors; but are the same system timing errors seen by the mobile units. The assumption is that any temporal variation in the ASF values is the same at both the reference station and the mobile unit. Thus by subtracting the ASF^* values of the fixed reference site from the measured ASF^* values, the timing errors and temporal variations cancel out leaving us with the true ASF difference between the reference site and the mobile location.

$$ASF^*(x, y, t) - ASF^*(x_{ref}, y_{ref}, t) = \Delta ASF(x, y)$$

This gives us a set of delta ASF values. Although we do not know the true ASF at every location, we do know the ASF variation, which allows us to look at the ASF gradients in the area of an airport. It is the magnitude of these gradients that is important in order to assess the feasibility of using a single airport ASF value to meet RNP 0.3.

The BALOR model calculates pure ASF values for each location (no timing errors or temporal variations) while our measurements are converted to relative ASF values. In order to compare the two, we must add a fixed offset value or bias term to the relative ASF values. If we wanted a true ASF grid, we would use the average ASF value from the reference station as this bias term. Since we have not yet evaluated whether the BALOR model has absolute accuracy or whether it is biased, we selected a bias term to put the relative values into the same range as the BALOR values. This allows us to see how well the BALOR model tracks the ASF gradients.

BALOR Model Performance

We used both types of data (ground measurements and flight measurements) to compare to the BALOR model. For the ground measurements we compared the relative ASFs to the BALOR predicted values for those specific points as described above. Figures 20 – 22 show this comparison for the Colorado test area for Loran Stations Gillette, Boise City, and Searchlight. In Colorado, there were three days worth of ground measurements (the most of any test area); one day each in the areas around each airport (Grand Junction, Montrose, and Rifle). If ordered by Latitude, there are no overlaps, so all plots are of ASF vs. Latitude. The points farthest South (smallest Latitude values) are the data collected around Montrose, the points in the middle are around Grand Junction, and those farthest North (largest Latitude values) are around Rifle. Refer back to Figure 18 for the specific locations on the map.

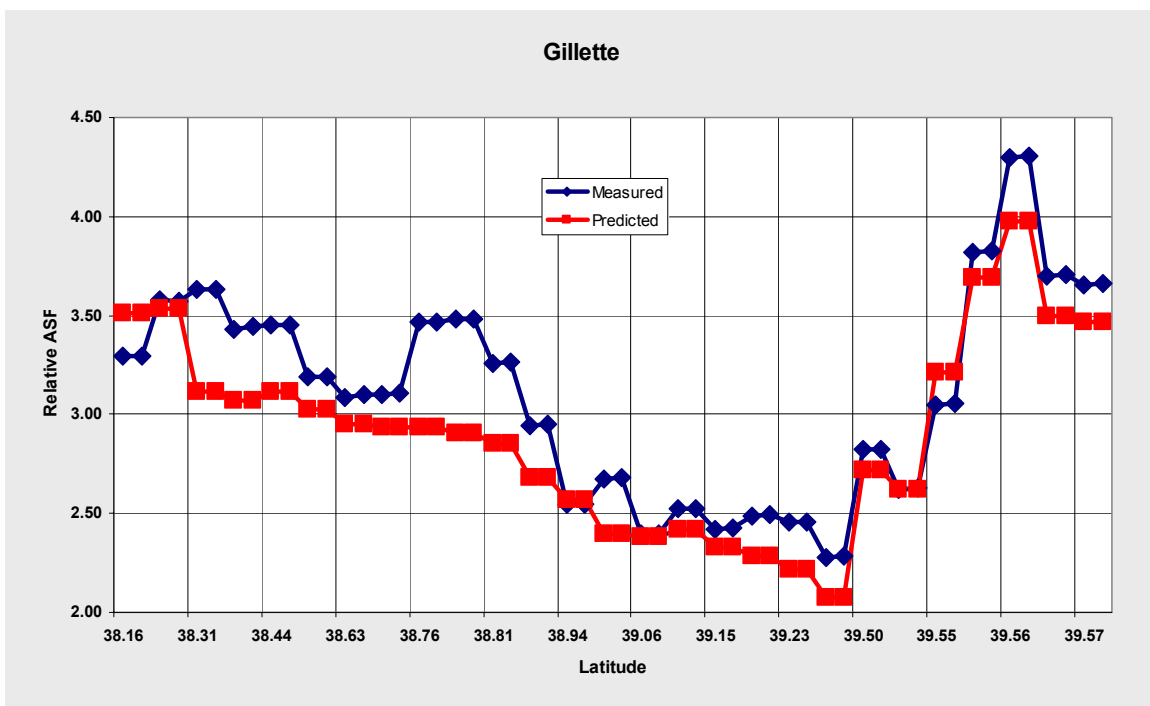


Figure 20 – Measured (blue) vs. predicted (red) ASFs for ground locations in Colorado, Loran Station Gillette, WY

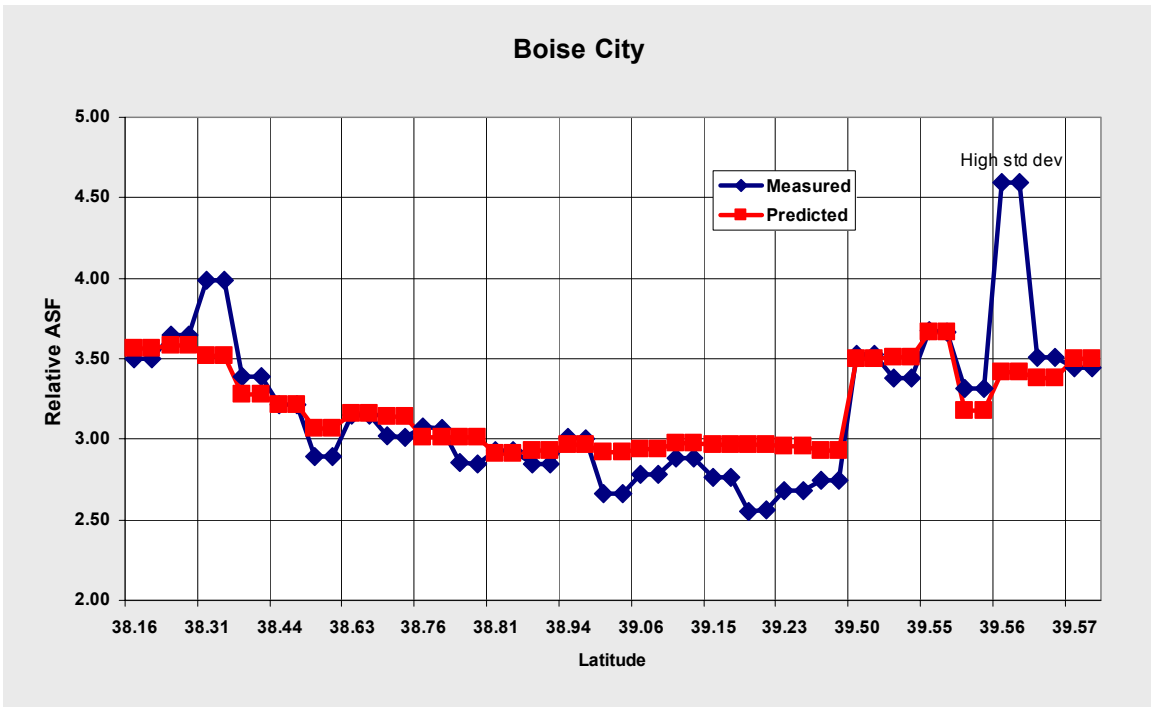


Figure 21 – Measured (blue) vs. predicted (red) ASFs for ground locations in Colorado, Loran Station Boise City, OK

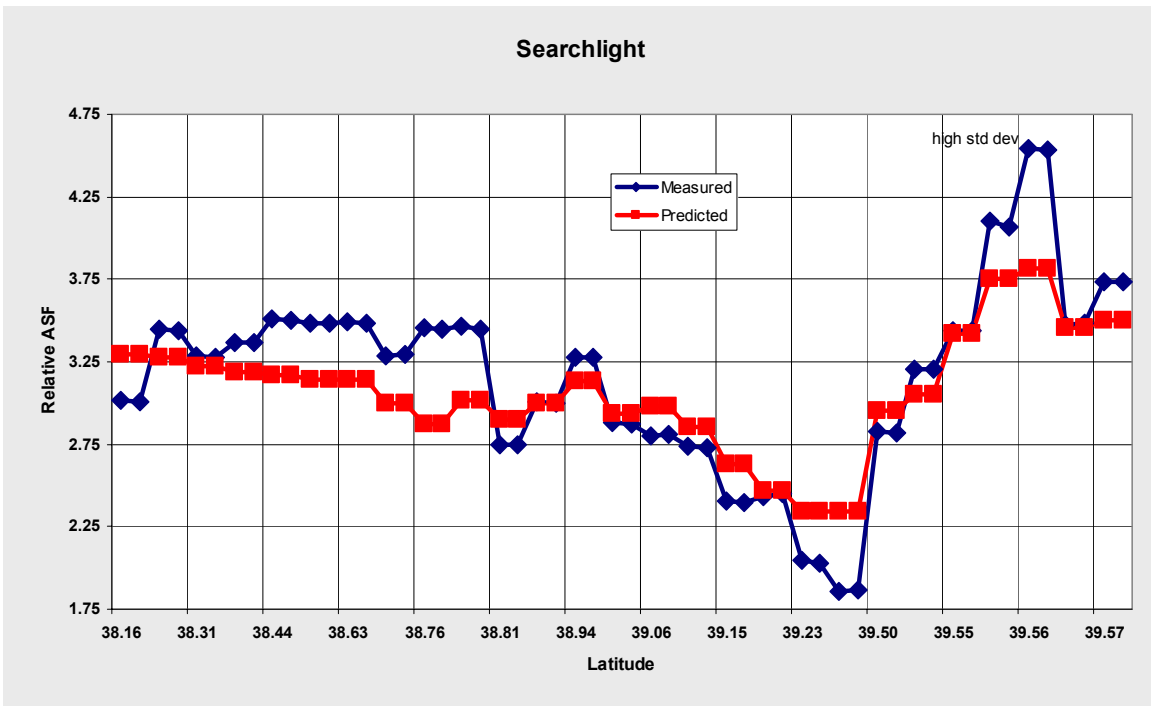


Figure 22 – Measured (blue) vs. predicted (red) ASFs for ground locations in Colorado, Loran Station Searchlight, NV

In each of these examples, it appears that the BALOR predictions track the measured values fairly well. In Figures 21 and 22, in the two locations that did not match well, the measured data suffered from excessive noise as seen by the high standard deviation of the measurements. These are probably poor measurement values. As expected, the BALOR model does not track ASF changes as rapidly as they may actually occur in real-life. This is due in part to the poor resolution of the conductivity database available (16km grid spacing).

Due to the difficulties in using the BALOR model to generate predictions for a flight profile we needed to use a test area where the ground was fairly flat under the flight area. Under these conditions the use of a single height above ground value in the BALOR model for the entire grid would be accurate. The California test area met these criteria. The flights in the cross patterns were either over the ocean or in the coastal area which is very low, 200-300 ft above sea level. The mountains do not start until further inland. Figure 23 shows all of the flight tracks (red, yellow, and green) for California, as well as the ground measurement locations (blue flags). For comparison purposes, we have chosen the flight corresponding to the red track.



Figure 23 – ASF measurement points in California; red, yellow, and green are flight paths; blue flags are ground measurement locations

In the comparison plots (Figures 24-27), the red cross pattern is separated into North-South legs and East-West legs as these were over the same path. In each case, the ASF difference due to the 180 degree heading difference disappears in the choice of a bias term for the comparison to the

predicted values. In each figure the BALOR predicted values are shown in dark blue. These values were pulled from the grid by interpolation based upon the GPS position of the aircraft's track. The BALOR predicted values based upon a grid at aircraft altitude is shown in black, but for this area, there was virtually no difference between the two grids so the BALOR lines plot on top of each other. There are four plots of measured values as the aircraft flew each leg twice in each reciprocal direction. The comparison is made for two different Loran Stations; Fallon, NV and Middletown, CA. For the East-West legs, the ASF values are plotted vs. Longitude. For the North-South legs, they are plotted vs. Latitude.

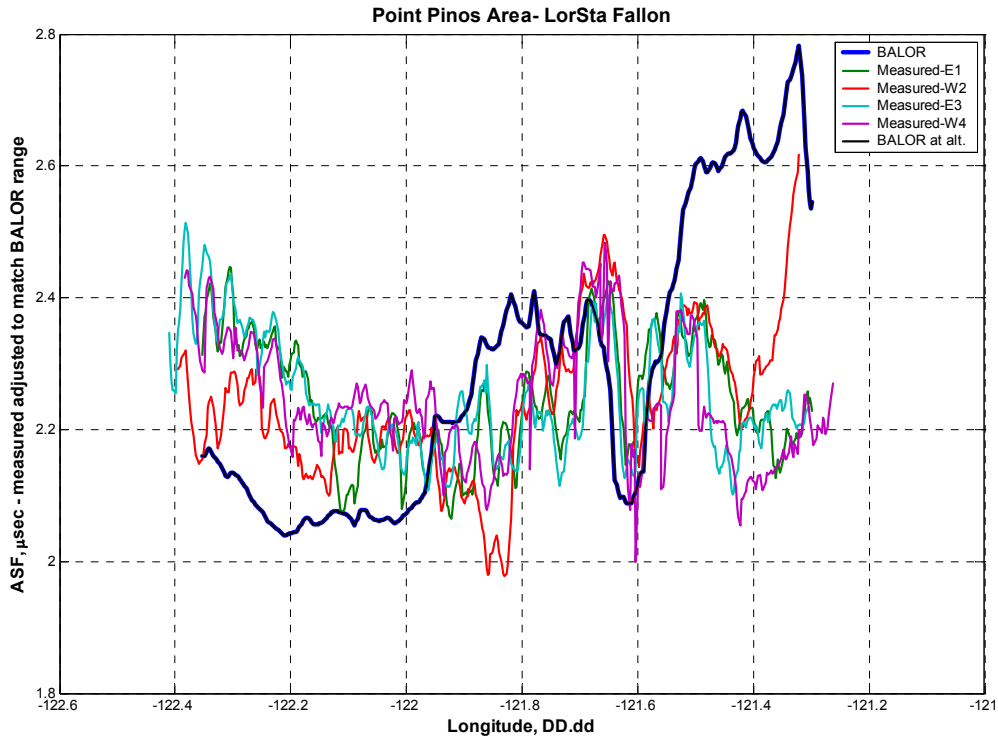


Figure 24 – Measured vs. predicted ASFs for East-West flight legs, Loran Station Fallon, NV

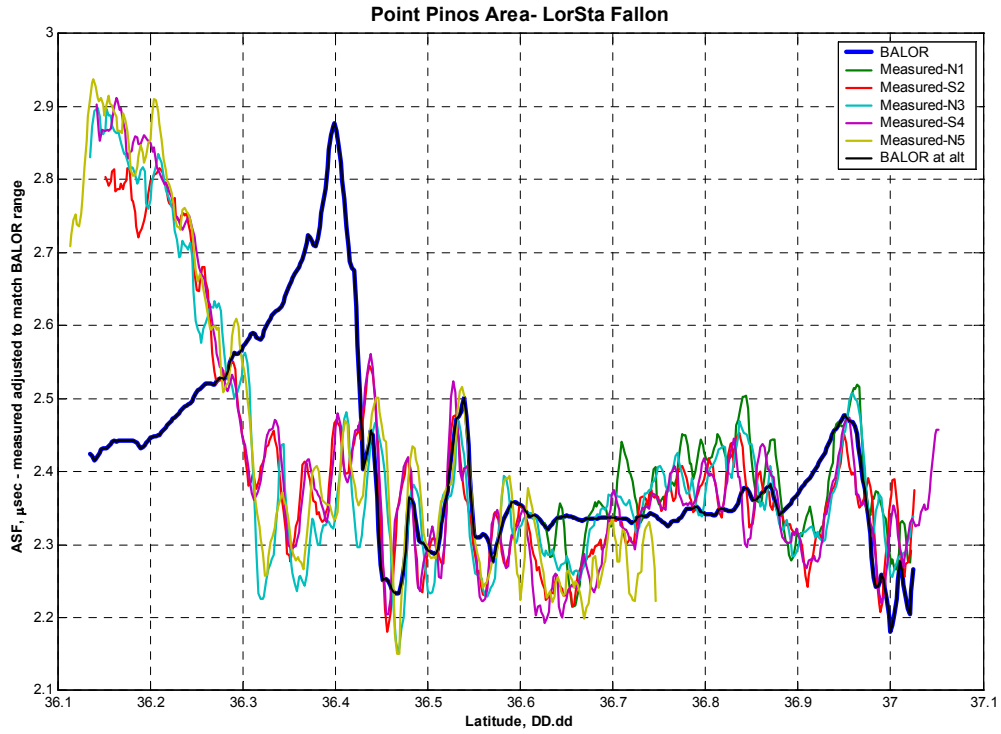


Figure 25 – Measured vs. predicted ASFs for North-South flight legs, Loran Station Fallon, NV

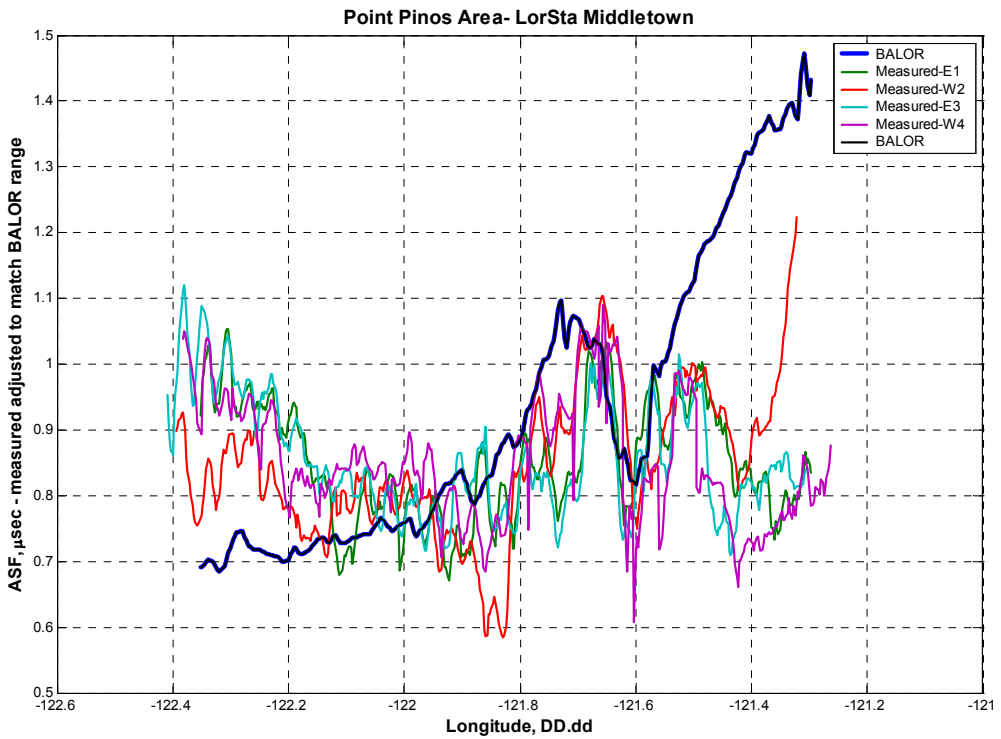


Figure 26 – Measured vs. predicted ASFs for East-West flight legs, Loran Station Middletown, CA

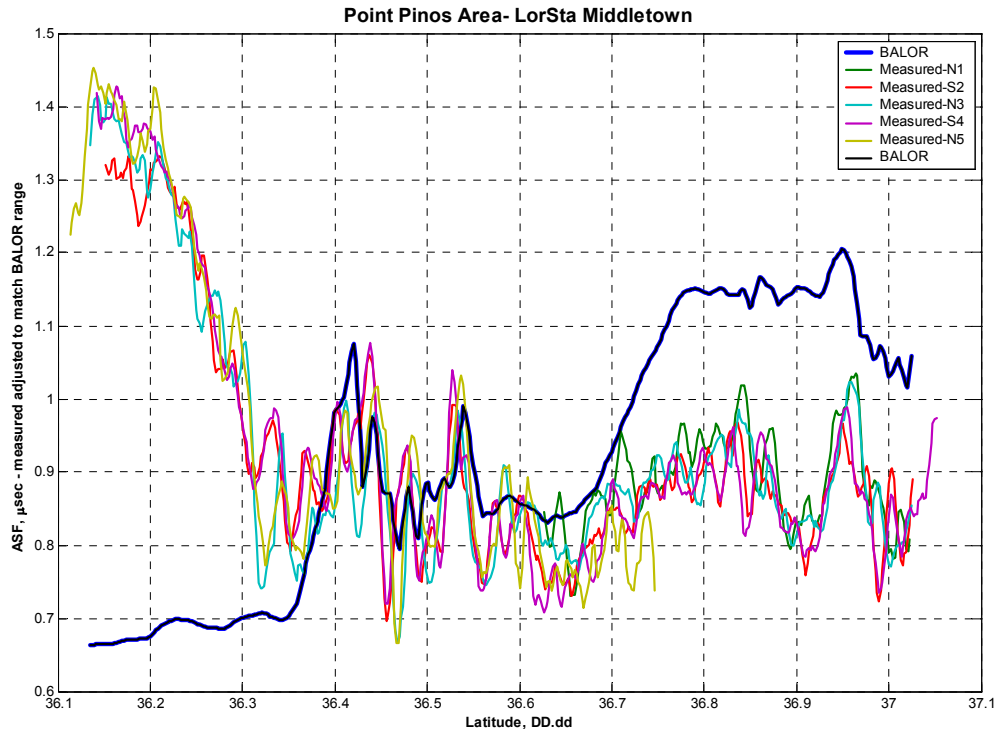


Figure 27 – Measured vs. predicted ASFs for North-South flight legs, Loran Station Middletown, CA

In each case, you can observe that the model tracks fairly closely in the middle of the legs, but not at the endpoints. Some of this is probably due to the fact that the model was designed to calculate ASFs at ground level and may not work properly at high altitudes.

Conclusions

Based upon our work to date, it appears that the BALOR model works reasonably well. The comparison to the ground level points is pretty good. The altitude performance (comparison to flight tracks) is less good and the model needs to be analyzed and possibly altered to correctly model these circumstances. We also still need to assess the bias in the model; i.e. how close are the actual ASF values to truth, or is there an offset that needs to be calibrated out of the model. The model however, does seem to be suitable to assess the gradients in the vicinity of an airport. This will be an important capability as it is not practical to measure the ASF gradients in the vicinity of every airport that would like a Loran NPA.

Further analysis of the data will continue in order to assess position performance using a single set of ASF values (one for each Loran tower) for each airport.

Acknowledgements

The authors would like to thank the sponsor of this work, Mr. Mitch Narins, FAA AND, the FAA Technical Center who provided the plane and the pilots, and the members of the JJMA Team that collected the data and provided support to the project; Mr. Christian Oates, Mr. George Sanders, Mr. Tim Waldie, and Mr. Ken Dykstra.

References

- [1] "Navigation and Landing Transition Strategy, 2002," Office of Architecture and Investment Analysis, ASD-1, Federal Aviation Administration, Washington, DC 2002.
- [2] R. Hartnett, G. Johnson, P. F. Swaszek, and M. J. Narins, "A Preliminary Study of LORAN-C Additional Secondary Factor (ASF) Variations," presented at 31st Annual Meeting, International Loran Association, Washington, DC, 2002.
- [3] G. Johnson, R. Hartnett, P. Swaszek, K. Gross, C. Oates, and M. Narins, "FAA Loran-C Propagation Studies," presented at Annual Technical Meeting, Institute of Navigation, Anaheim, CA, 2003.
- [4] R. Hartnett, G. Johnson, P. F. Swaszek, and K. Dykstra, "Getting a Bearing on ASF Directional Corrections," presented at 32nd Annual Meeting, International Loran Association, Boulder, CO, 2003.
- [5] P. Swaszek, G. Johnson, C. Oates, R. Hartnett, and G. Weeks, "A Demonstration of High Accuracy Loran-C for Harbor Entrance and Approach Areas," presented at Fifty-ninth Annual Meeting, Institute of Navigation, Albuquerque, NM, 2003.
- [6] D. Last and P. Williams, "Loran-C ASF, Field Strength and ECD Modelling," presented at LORIPP meeting, Tysons Corner, VA, 2003.
- [7] P. Williams and D. Last, "Mapping the ASFs of the Northwest European Loran-C System," presented at 28th Annual Convention and Technical Symposium, International Loran Association, 1999.

DISCLAIMER AND NOTE

The views expressed herein are those of the authors and are not to be construed as official or reflecting the views of the Commandant, the U.S. Coast Guard, the Federal Aviation Administration, or any agency of the U.S. Government.